Four Enantiomerization Routes of 1,2,2-Trimesitylvinyl Acetate. Enantioselective Liquid Chromatography of (*E*)- and (*Z*)-2-*m*-Methoxymesityl-1,2-dimesitylvinyl Acetates

Elimelech Rochlin,[†] Zvi Rappoport,*[,†] Fritz Kastner,[‡] Nikola Pustet,[‡] and Albrecht Mannschreck[‡]

Department of Organic Chemistry, The Hebrew University, Jerusalem 91904, Israel, and Institut für Organische Chemie der Universität, Universitätstrasse 31, D-93040, Regensburg, FRG

Received June 29, 1999

The vinyl propellers (*E*)- and (*Z*)-2-*m*-methoxymesityl-1,2-dimesitylvinyl acetates (**3c** and **3d**) were prepared and their geometries assigned. The stereoisomerization barriers of the trimesityl vinyl acetate system were determined by DNMR and by enantioselective LC resolution and polarimetric monitoring of the behavior of the two diastereomeric racemates of **3c** and **3d**. Combined with data for trimesitylvinyl-OAc **3a** and its 1-*m*-methoxymesityl analogue **3b**, the following order of barriers $\Delta G^{\ddagger}$ is obtained: $\alpha\beta$-2-ring flip > $\alpha\beta'$-2-ring flip > $\beta\beta'$-2-ring flip > $\alpha\beta\beta'$-3-ring flip (the threshold enantiomerization barrier). This order which differs from the previously found orders for trimesitylvinyl-X, X = H, OPr-*i* was rationalized and discussed.

Triarylvinyl systems exist in the solid state and in solution in a chiral propeller conformation, and the static and dynamic stereochemistry of these triarylvinyl propellers were studied extensively during the past decade.[1] The stereoisomerization pathways in triarylvinyl propellers were described[1,2] in terms of "flip" processes.[3] In a flip process the flipping ring passes during the rotation via a plane perpendicular to the double bond plane, while concurrently nonflipping rings pass via the C=C plane. The mechanism is designated by the number of the flipping rings. Thus, for a triarylvinyl propeller where each ring has C_2 symmetry, one 0-ring flip, three isomeric 1-ring flips, three isomeric 2-ring flips, and one 3-ring flip, all leading to enantiomerization, are possible. Figure 1 displays the four latter pathways with the corresponding transition states for a tris(*o*,*o*′-dimethylphenyl)vinyl-X system. However, the experimental data on the barriers ($\Delta G^{\ddagger}$) for the different alternative enantiomerization routes in a single system are limited to two systems **1** and **2**. Two competing enantiomerization routes were reported for 1,2,2-trimesitylethylene **1**[4] where the order of the barriers was $\Delta G^{\ddagger}_{\alpha\beta\beta'} > \Delta G^{\ddagger}_{\alpha\beta}$, where the subscripts indicate the flipping rings in the transition state of the enantiomerization.

$Mes_2C{=}CHMe$

1

Mes = Mesityl =2,4,6-trimethylphenyl

In a previous study the dynamic stereochemistry of 1,2,2-trimesitylvinyl isopropyl ethers **2a**−**d**[5] was investigated. The activation barriers for the four enantiomerization routes depicted in Figure 1 were measured by a DNMR technique by labeling one at a time each of the mesityl rings by a *m*-OMe group, which converts the $\alpha\beta\beta'$-3-ring flip enantiomerization route to a diastereomeriza-

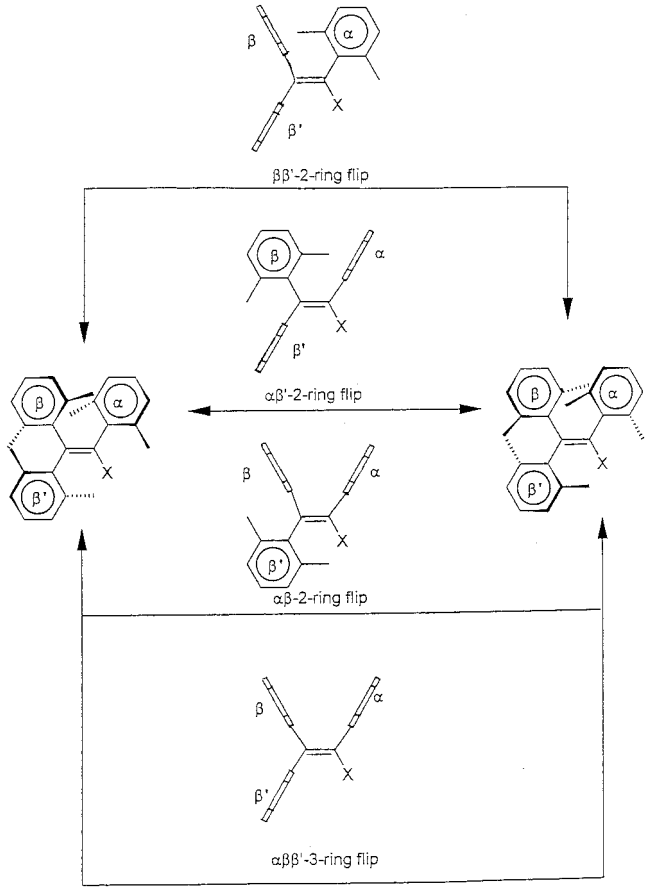

Figure 1. Four enantiomerization routes and idealized transition state structures of a triarylvinyl propeller. The structures in the middle are the corresponding transition states with the rings either in the C=C plane or perpendicular to it.

[†] The Hebrew University.
[‡] Institut für Organische Chemie der Universität, Regensburg.

(1) Rappoport, Z.; Biali, S. E. *Acc. Chem. Res.* **1997**, *30*, 307.
(2) Biali, S. E.; Rappoport, Z. *J. Am. Chem. Soc.* **1984**, *106*, 477.
(3) (a) Kurland, R. J.; Schuster, I. I.; Colter, A. K. *J. Am. Chem. Soc.* **1965**, *87*, 2276. (b) Mislow, K. *Acc. Chem. Res.* **1976**, *9*, 26. (c) Mislow, K.; Gust, D.; Finocchiaro, P.; Boettcher, R. J. *Topics in Current Chemistry, No 47, Stereochemistry 1*; Springer-Verlag: Berlin, 1974; p 1.
(4) Biali, S. E.; Rappoport, Z. *J. Org. Chem.* **1986**, *51*, 2245.
(5) Rochlin, E.; Rappoport, Z. *J. Org. Chem.* **1994**, *59*, 3857.

10.1021/jo9910435 CCC: $18.00
Published on Web 10/30/1999

tion route. It was shown that the OMe labeling affects only slightly the energy of both the ground and the transition states. However, this susbstitution makes "visible" the routes having higher energies than that for the threshold process (which are invisible in the nonlabeled system) by reducing the symmetry of the threshold transition state. The order of the observed barriers for system **2** was $\Delta G^{\ddagger}_{\beta\beta'} > \Delta G^{\ddagger}_{\alpha\beta} > \Delta G^{\ddagger}_{\alpha\beta'} > \Delta G^{\ddagger}_{\alpha\beta\beta'}$. This order was corroborated by MM2 calculations and was rationalized by analysis of the steric interactions in the different transition states.

Therefore, the order of the enantiomerization barriers differs even in these two trimesitylvinyl propellers. Consequently, a study of additional trimesitylvinyl systems is desired in order to delineate the structural factors that govern the relative order of the barriers.

In the present paper we extend our previous studies[2,6] of the different enantiomerization routes in 1,2,2-trimesitylvinyl acetate **3a** by applying a similar labeling technique with a *m*-OMe group one at a time for each of the mesityl rings, thus generating **3b**−**d**. In contrast with the work on **2a**−**d** and **3a** which applied only the DNMR technique, in the present work we achieved resolution of enantiomeric pairs of **3c** and **3d** by enantioselective LC and applied a stop-flow on-line chiroptical detection[7] in order to follow the stereoisomerization processes. This resembles the previous study of **3b**.[6] This method was supplemented by using the DNMR technique in order to independently corroborate the measured values of the threshold barriers.

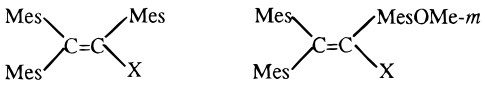

2a: X = OPr-*i* **2b**: X = OPr-*i*
3a: X = OAc **3b**: X = OAc

m-MeOMes = 3-MeO-2,4,6-Me_3C_6H

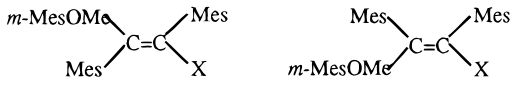

2c: X = OPr-*i* **2d**: X = OPr-*i*
3c: X = OAc **3d** : X = OAc
4c: X = OH **4d** : X = OH

Results and Discussion

Synthesis and Geometry Assignment of 3c and 3d. The two geometrical isomers (*E*)- and (*Z*)-2-*m*-methoxymesityl-1,2-dimesitylvinyl acetates (**3c** and **3d**) were synthesized by acetylation and subsequent chromatographic separation of a mixture of the corresponding enols, (*E*)- and (*Z*)-2-*m*-methoxymesityl-1,2-dimesitylethenols **4c** and **4d** which were prepared earlier.[5] The configurations of **3c** and **3d** were assigned on the basis of the near correspondence between the δ(MeO) values in the enols (**4**) and the ethers (**2**) of known configuration[5] and the acetates (**3**) in $CDCl_3$. For **4c** δ(MeO) = 3.29 (major diastereomer), 3.52 (minor diastereomer); for **2c** δ(MeO) = 3.26 (major diastereomer), 3.50 (minor diastereomer). The *E*-geometry of **4c** and **2c** was determined unequivocally by X-ray diffraction.[5] The values δ(MeO) = 3.29 (major diastereomer), 3.53 (minor diastereomer) for **3c**, indicate its *E*-structure. For the isomers having the *Z*-geometry, δ(MeO) = 3.59 (minor diastereomer), 3.75 (major diastereomer) for **4d**, and 3.54 (minor diastereomer), 3.76 (major diastereomer) for **2d**. Hence, the values δ(MeO) = 3.56 (minor diastereomer) and 3.73 (major diastereomer) indicate a *Z*-structure for **3d**. The generalization that the more stable *E*-diastereomer displays the lower δ(MeO) value and the more stable *Z*-diastereomer displays the higher δ(MeO) value is in line with the MM calculations which show that in the most stable structure of both isomers the MeO group faces the *cis* vicinal group.[5] In the *E*-isomer this group is Mes, and the MeO is at the shielding zone of the α-ring, while in the *Z*-isomer it is the X group (X = H, OPr-*i*, AcO) and a shielding effect is absent.

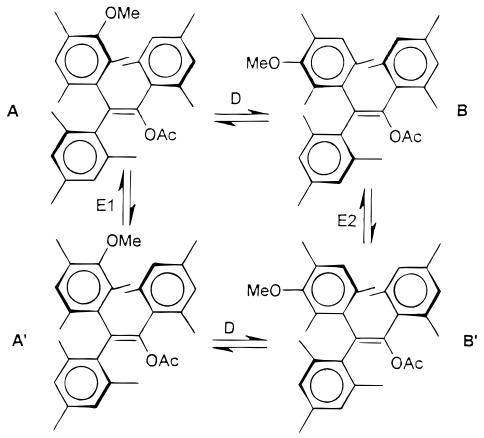

Figure 2. Isomerization routes of acetate **3c**. D: A diastereomerization 3-ring flip process; E1, E2: two isomeric enantiomerization 2-ring flip processes.

Static and Dynamic NMR Study. Each one of the molecules **3c** and **3d** exists in solution as a mixture of two enantiomeric pairs (Figure 2). For a "frozen" conformation on the NMR time scale in the absence of signals overlap, either **3c** or **3d** should show 2 MeO singlets, 18 mesityl-Me, 2 acetyl-Me, and 10 mesityl-H singlets. The static ^{1}H NMR spectra in $CDCl_3$ at room-temperature corroborate this prediction (see Experimental Section). In $C_6N_5NO_2$ at room temperature **3c** displays two MeO singlets in a 2:1 ratio, with $\Delta\nu$ = 42.4 Hz. The diastereomerization barrier was evaluated by the DNMR method, similarly to that previously used.[2−6] On raising the temperature the two MeO signals are broadened and finally coalesce. In monitoring the DNMR behavior the OMe signal serves as a probe, giving the threshold 3-ring flip diastereomerization barrier of 19.7 kcal mol^{-1} at the coalescence temperature of 121.5 °C. Similarly, **3d** displays at room temperature two MeO singlets with a 1:2 ratio and $\Delta\nu$ = 73.4 Hz. They coalesce at 112.3 °C, giving a $\Delta G^{\ddagger}$ of 18.8 kcal mol^{-1}. Barriers of 19.0 kcal mol^{-1} for the enantiomerization of **3a** and the diastereomerization of **3b** were obtained previously.[2,6]

Liquid Chromatography Resolution and Stereoisomerization Barriers. To evaluate the different 2-ring flip enantiomerization barriers, which must be substantially higher than these threshold values,[5,6] a

(6) Biali, S. E.; Rappoport, Z.; Mannschreck, A.; Pustet, N. *Angew. Chem., Int. Ed. Engl.* **1989**, *28*, 199.
(7) (a) Brandl, G.; Kastner, F.; Fritsch, R.; Zinner, H.; Mannschreck, A. *Monatsh. Chem*. **1992**, 123, 1059. (b) Mannschreck, A. *Trends Anal. Chem*. **1993**, *12*, 220; *Chem. Abstr*. **1993**, *119*, 194725.

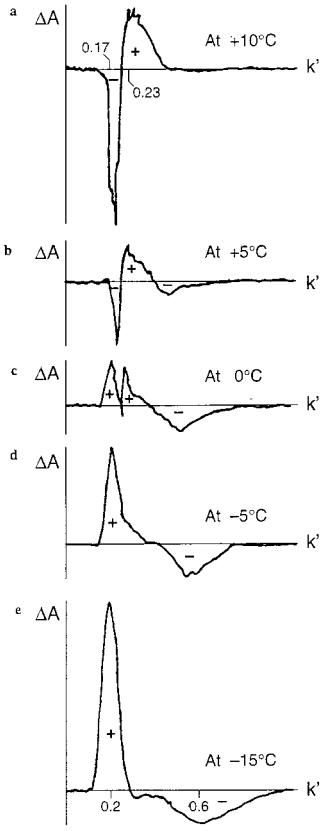

Figure 3. Chromatograms of **3c** in differential absorption Δ*A* scale at 290 nm at different temperatures.

previously described technique[6,7] was used. Attempted resolutions of racemates of **3c** and **3d** were tried on different enantioselective LC columns. The best resolutions were achieved on tris(phenylcarbamoyl)cellulose/SiO_2 (Carbamate) and (+)-poly(trityl methacrylate)/SiO_2 columns using EtOH and MeOH, respectively, as eluents. In both cases, in the range from +10 °C up to room temperature the chromatograms of either **3c** or **3d** look as one partly separated racemate, i.e., either as two peaks or as a one broad peak with (−) and (+) halves in circular dichroism (CD) detection (Figure 3a). On decreasing the temperature to +5 °C, the peaks were "doubled", i.e., a small (+) peak appears before the (−) half and a small (−) peak follows the (+) half (Figure 3b). This "splitting" becomes more pronounced as the temperature is further decreased: in the 0 °C range four peaks (for the two racemates) are observed, appearing in the order (+)(−)(+)(−) (Figure 3c). On further temperature decrease to −15 °C the chromatogram once again resembles that of a single racemate, but with an opposite order of the halves, i.e., (+)(−) (Figures 3c and 3d). A spectrum similar to that of Figure 3e was observed at −25 °C. Consequently, it seems that the "dynamic" chromatogram at +10 °C displays a single separated racemate that is converted at −25 °C to another racemate, whereas the two racemates exist together at intermediate temperatures. The suggestion that two different racemates are apparently separated at +10 °C and at −25 °C is supported by the following experiments: The eluate was trapped in the dichrograph cell at +10 °C at point 1 (Figures 4a and 5a) by stopping elution, and a CD spectrum was recorded. The elution was then continued and the same procedure repeated at point 2 (Figures 4a and 5a). The two CD spectra obtained were found to be of opposite signs; the intensity differences are due to different concentrations at points 1 and 2 (Figures 4 and 5). When the same procedure was repeated at −25 °C (Figures 4b and 5b, points 1 and 2), two CD spectra showing opposite signs, but completely different appearance from the former spectra, were obtained (Figures 4b and 5b).

We tentatively attribute this behavior to the composition of our stereoisomeric mixture (Figure 2). We expect to have in the mixture four stereoisomers A, A′, B, and B′ that differ either by their helicity (right- or left-handed) or by the orientation of the OMe group (above or below the plane of the C═C double bond) or by both. Hence, if a maximum resolution is achieved, we expect

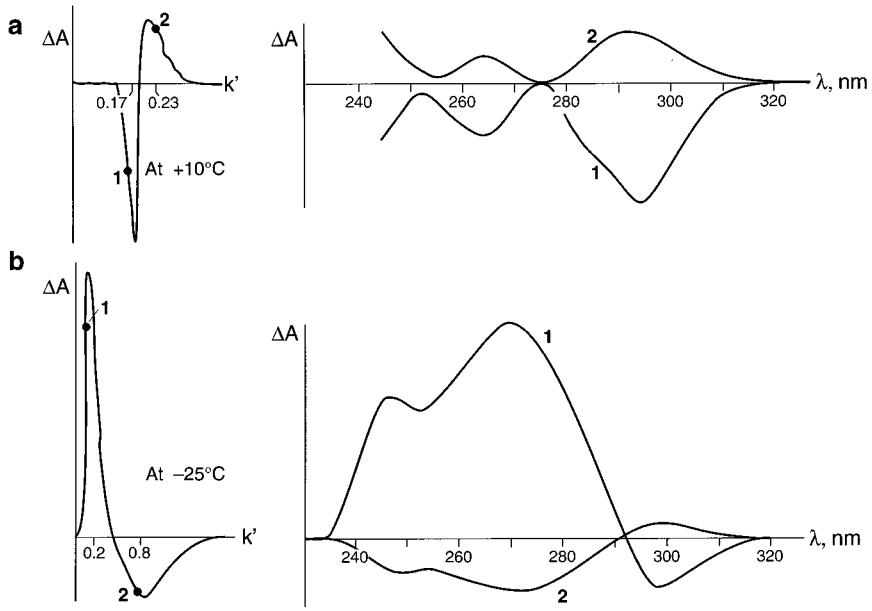

Figure 4. (a) Left: A chromatogram of **3c** at 290 nm at +10 °C. **1** and **2** were collected at the points indicated. Right: CD spectra of samples **1** and **2**. (b) Left: A chromatogram of **3c** at 290 nm at −25 °C. **1** and **2** were collected at the points indicated. right: CD spectra of samples **1** and **2**.

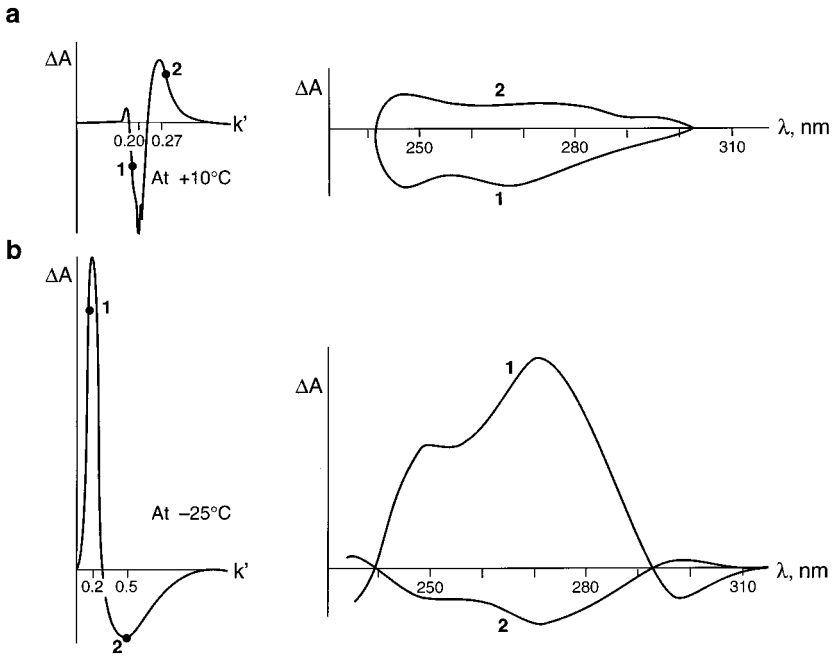

Figure 5. (a) Left: A chromatogram of **3d** at 290 nm at +10 °C. **1** and **2** were collected at the points indicated. Right: CD spectra of samples **1** and **2**. (b) Left: A chromatogram of **3d** at 290 nm at −25 °C. **1** and **2** were collected at the points indicated. Right: CD spectra of samples **1** and **2**.

to observe four components on the chromatogram, and this is what we observe at intermediate temperatures (+5° to −10 °C). At incomplete resolution peaks due to two different partly resolved racemates could be combined to give (AB)(A′B′) or (AB′)(A′B). The residual enantiomerism is due to the orientation of the MeO group in the former racemate, whereas it is due to the helicity direction in the latter racemate. We expect different chiroptical properties of the two racemates, as is indeed observed at the two extreme temperatures +10 °C and −25 °C. It is conceivable that the four retention factors k' of the four species on the chiral column may show a different response to a change in the temperature, accounting in this way for the observed temperature changes. An alternative explanation ascribing the observed changes to a change in the population of diastereomeric A and B (A′ and B′) pairs is unlikely for two reasons. (i) It cannot explain the observed changes at all temperatures. (ii) A study of stereoisomeric mixtures of **3c** and **3d** in CD_3OD by ^1H NMR at +22° to −68 °C showed that the equilibrium constant $K = [A]/[B]$ is only slightly temperature-dependent; e.g., for **3c** $K = 2.02$ at +22 °C, 2.25 at −8 °C, and 2.31 at −68 °C.

If our interpretation is correct it raises a rare opportunity to measure consecutively both the 3-ring flip diastereomerization barrier and a 2-ring flip enantiomerization barrier in the same solution by using the same peak. The reason is that the 2-ring flip barrier must be 3−6 kcal mol^{-1} higher than the 3-ring flip barrier.[5,6] If we trap a species which shows one of the four peaks at −10 °C in the polarimetric cell, the measured change in the rotation angle will be mainly (or entirely) due to the faster process, i.e., to the 3-ring flip. If the temperature is then raised, this process will be rapidly completed and further changes will be due to the slower 2-ring flip process. This was indeed realized by the stopped-flow online technique. The solutions of **3c** and **3d** were eluted from the Carbamate column which was thermostated at −10 °C. When one of the peaks was detected in the polarimetric cell, the flow stopped and the change of α as a function of time was recorded in the thermostated cell at −10 °C. The cell was then heated to +31.8 °C in the experiment with **3c** and to +67 °C in the experiment with **3d** and the α vs time curves were recorded. First-order kinetic plots were obtained in all the cases. The derived first-order polarimetric and stereoisomerization (i.e., enantiomerization and diastereomerization) rate constants and the respective stereoisomerization barriers are summarized in Table 1. The enantiomerization rate constants ($k_{enantio}$) were obtained from the polarimetric rate constants (k_{pol}) by using a statistical correction of 2, i.e., $k_{pol} = 2k_{enantio}$. The diastereomerization rate constants were obtained by dividing k_{pol} by $(K + 1)/K$ for the reaction in one direction or by $K + 1$ for the reaction in the opposite direction, where K (= 2.2 for **3c**, and 2.3 for **3d**) is the equilibrium constant for the two diastereomers measured by NMR at the same temperature and solvent. The 3-ring flip diastereomerization barrier for **3c** thus obtained (19.6 kcal mol^{-1}) is similar to the value evalu-

Table 1. Polarimetric (k_{pol}) and Stereoisomerization ($k_{stereo} = k_{enantio}$ or $k_{diastereo}$) Rate Constants and Barriers for 3c and 3d in EtOH[a]

compound	column temp, °C	cell temp, °C	$10^5 k_{pol}$, s^{-1}	$10^5 k_{enantio}$ or $10^5 k_{diastereo}$, s^{-1}	$\Delta G^{\ddagger}_{enantio}$ or $\Delta G^{\ddagger}_{diastereo}$ kcal mol^{-1},[b]
3c	−10	−10	38	26[d]	19.6[d]
				12[d]	20.0[d]
	−10	−10	36	25[d]	19.6[d]
				11[c]	20.0[d]
	−10	+31.8	24.6	12.3[c]	23.3[c]
3d	−10	−10	48	33[d]	19.5[d]
				14.5[d]	19.9[d]
	−10	−10	46	32[d]	19.5[d]
				14[d]	19.9[d]
	−10	+67.0	3.7	1.85[c]	27.3[c]
	+20	+67.5	3.9	1.95[c]	27.3[c]

[a] Obtained by the stopped-flow technique, on line with a polarimeter, after LC on Carbamate column (see text). [b] Values ± 0.1 kcal mol^{-1}. [c] $k_{enantio}$. [d] $k_{diastereo}$.

Table 2. Rotational Barriers for the Various Flip Processes ($\Delta G^{\ddagger}$) and Several Bond Lengths (from X-ray data) for Several $Mes_2C{=}C(X)Mes$ Systems

	$\Delta G^{\ddagger}$, kcal mol^{-1}				bond length, Å			
X	$\alpha\beta\beta'$	$\alpha\beta$	$\alpha\beta'$	$\beta\beta'$	C1−C2	C1−Ar_α	C2−Ar_β	C2−$Ar_{\beta'}$
OPr-*i*[9]	15.8	23.1	21.1	25.2	1.354	1.498	1.506	1.52
H	20.5[4] (18.3[a])	16.8[4] (15.4[a])	19.9[a]	21.0[a]	1.343[8]	1.48[8]	1.517[8]	1.497[8]
OAc	19.0[2]	27.3	23.3	22.2[6]	1.33[2]	1.51[2]	1.48[2]	1.48[2]

[a] MM2 calculated value.[5]

ated from the DNMR experiments (19.7 kcal mol^{-1}) despite the substantially different temperature of these measurements (−10 °C for the polarimetry and +121.5 °C for the coalescence in the DNMR). However, there is a 0.7 kcal mol^{-1} difference between the polarimetric and DNMR values for **3d** (19.5 and 18.8 kcal mol^{-1}, respectively).

Relative Stereoisomerization Barriers in the Trimesitylvinyl-X System. We now have a number of values (in kcal mol^{-1}) for the 3-ring flip barrier of trimesitylvinyl acetates **3a**−**d**: 19.0 (**3a**),[2] 19.0 (**3b**),[6] 19.6 (**3c**), and 18.8−19.5 (**3d**). More important, together with earlier data for **3b**[6] the following higher energy barriers (in kcal mol^{-1}) are available for three different 2-ring flips: 22.2 for the $\beta\beta'$-2-ring flip of **3b**, 23.3 for the $\alpha\beta'$-2-ring flip of **3c**, and 27.3 for the $\alpha\beta$-2-ring flip of **3d**.

If we assume that the effect of the remote *m*-methoxy group on the 2-ring flip barriers of **3a** is small, as found for the corresponding barriers for **2a**−**d**[2,5] or for the 3-ring flip barrier of **3a**−**d**, then the observed order for the different enantiomerization routes of trimesitylvinyl acetate is $\Delta G^{\ddagger}_{\alpha\beta} > \Delta G^{\ddagger}_{\alpha\beta'} > \Delta G^{\ddagger}_{\beta\beta'} > \Delta G^{\ddagger}_{\alpha\beta\beta'}$. This order differs from that obtained either for trimesitylvinyl isopropyl ether[5] or for trimesitylvinylethylene (Table 2).[4] Consequently, the order of activation barriers for the different enantiomerization routes of the $Mes_2C{=}C(Mes)X$ system is not uniform and it depends on the nature of the vinyl substituent X. Hence, it is not easy to ascribe this substituent effect to a single factor, i.e., steric or electronic, which governs the order of the barriers in these systems. If other effects are neglected, the 4 kcal mol^{-1} higher enantiomerization barrier for **3c** than for **3d** could be ascribed to the higher steric interaction between the β'-aryl ring and the OAc group in the transition state of the $\alpha\beta$-2-ring flip, than between the β-aryl and the two perpendicular α-Ar and β'-Ar rings in the transition state of the $\alpha\beta'$-2-ring flip. Nevertheless, there are some structural−dynamic regularities based on the observed and MM2 calculated barriers[5] for the three systems **1**−**3** which are summarized together with several X-ray-determined bond lengths in Table 2,[2,5,6,8] that enable us to make some reasonable assumptions.

Inspection of Table 2 shows that the highest barrier for X = OAc is for the $\alpha\beta$-2-ring flip, in which the nonflipping ring which passes through double bond plane is connected to C2. The opposite applies for X = OPr-*i* and H, where the $\beta\beta'$-2-ring flip, in which the ring connected to C1 is nonflipping, has the highest barrier.

There are other differences: for X = OAc the C1−C2 double bond is the shortest among the three systems, whereas for X = OPr-*i* it is the longest. For X = OAc the longest C−Ar bond is C1−Ar_α, and C2−Ar_β and C2−$Ar_{\beta'}$ are identical and shorter. In contrast, the longest C−Ar bond is C2−$Ar_{\beta'}$ when X = OPr-*i* for **2a** or C2−Ar_β for **1** (X = H), whereas the shortest bond in both is C1−Ar_α.

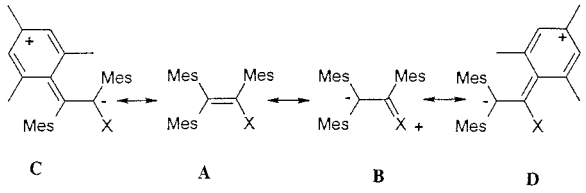

Figure 6. Valence bond zwitterionic structures A−D of the trimesitylvinyl-X system.

Inspection of the MM2-calculated transition state structures in our earlier work on systems **1** and **2**[5] shows that, in addition to the change in the torsion angles of the rings, one of the most remarkable structural changes in the transition state of the 2-ring flip process is a substantial elongation of the =C−Ar bond of the nonflipping ring. By using the principle of structural correlation,[9] we predict that in the absence of other effects, the system with the shortest =C−Ar bond in the ground state will have a higher activation barrier for the flip process in which this Ar ring is nonflipping (and vice versa). Accordingly, the higher energy 2-ring flip process when X = OPr-*i* will be the $\beta\beta'$-2-ring flip with a nonflipping α-ring, which is the lower energy process for X = OAc. The higher energy process for X = OAc must be either the $\alpha\beta$- or the $\alpha\beta'$-2-ring flip process, when a C2 aryl ring is nonflipping. The preference of some trimesitylvinyl systems for a higher energy $\alpha\beta$-2-ring flip process and for others for a $\beta\beta'$-2-ring process in the absence of large steric changes (this does not apply for X = H) may be ascribed to electronic effects. Electron-donating substituents will increase the contribution of structures with negatively charged C2 and positively charged C1 (cf. structures B and D in Figure 6). This, in turn, will elongate the C1−C2 bond and shorten the C1−Ar_α bond. It is unlikely that mesityl rings will substantially delocalize the negative charge, so that the C2−Ar_β and C2−$Ar_{\beta'}$ bonds will be longer than the C1−Ar_α bond. This will reduce the barriers for the $\alpha\beta$- and $\alpha\beta'$-2-ring flips and increase the barrier for the $\beta\beta'$-2-ring flip. The opposite is true for electron-withdrawing substituents where structures A and C (Figure 6) will be the main contributors and hence the C1−C2, C2−Ar_β, and C2−$Ar_{\beta'}$ bonds will be shortened with a consequent increase in the $\alpha\beta$- and $\alpha\beta'$-2-ring flip barriers and decrease of the $\beta\beta'$-2-ring flip barrier. Hence, electronic effects seem more important for the higher energy 2-ring flip processes than for the threshold 3-ring flip process.

Finally, the relatively high enantiomerization barrier for **3d** makes it a good candidate for a full preparative

(8) Kaftory, M.; Biali, S. E.; Rappoport, Z. *J. Am. Chem. Soc.* **1985**, *107*, 1701.

(9) (a) Bürgi, H. B. *Angew. Chem., Int. Ed. Engl.* **1975**, *14*, 460. (b) Dunitz, J. D. *X-ray Analysis and the Structure of Organic Molecules*; Cornell University Press: Ithaca, NY, 1979. (c) Bürgi, H. B.; Dunitz, J. D. *Acc. Chem. Res.* **1983**, *16*, 153.

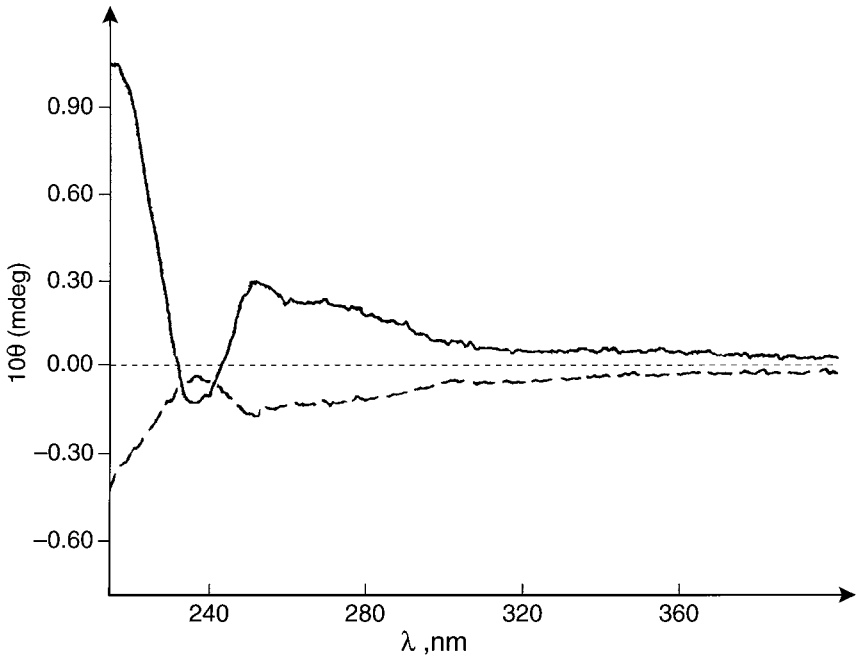

Figure 7. CD spectra in EtOH of the two enantiomers (5.10^{-5} mol L^{-1}) of **3d** after resolution.

resolution. This was indeed achieved on an Amylose tris-(3,5-dimethylphenylcarbamate) column.[10] The CD spectra of the two enantiomers are given in Figure 7.

Experimental Section

General Methods. Melting points are uncorrected. ^{1}H NMR spectra were recorded on a pulsed FT spectrometer operating at 400.266 MHz.

Solvents and Materials. Pyridine was kept for several days over KOH, distilled, and then stored over molecular sieves. Other solvents were commercial and were used without further purification.

Analytical Liquid Chromatography. The instruments and the columns were given earlier.[7a,11] The measurements of on-line CD spectra[7a] and kinetics of the stereoisomerizations by on-line polarimetry[11] were performed as previously described.

***(E)*/(*Z*)-2-(*m*-Methoxymesityl)-1,2-dimesitylvinyl Acetates (3c and 3d).** To a solution of mixture of enols **4c** and **4d**[5] (0.1 g, 0.23 mmol) in pyridine (0.5 mL) was added acetic anhydride (0.15 mL, 1.5 mmol), and the mixture was refluxed for 5 h, after which the reaction was complete (by TLC). The mixture was poured into water (25 mL), and concentrated HCl was added dropwise with stirring until the odor of pyridine disappeared. The mixture was extracted with ether (20 mL), dried ($MgSO_4$), and evaporated, yielding a yellow oil (97 mg, 90%) which according to the ^{1}H NMR spectrum is a mixture of the (*E*)- and (*Z*)-vinyl acetates. The isomers were separated by chromatography on a silica column (230−400 mesh) using consecutively petroleum ether and 1:1 petroleum ether−chloroform as the eluent. The *E*-isomer **3c** (49 mg, 45%), mp 119−120 °C, is eluted first, followed by the *Z*-isomer **3d**, mp 149−150 °C (from MeOH, 45 mg, 42%).

3c: λ_{max}(hexane): 213 nm (log ϵ 4.68), 240.5 (4.40), 280 (4.24). ^{1}H NMR ($CDCl_3$) shows two diastereomers of residual helicity in a 2.2 ratio with 25 out of the possible maximum of 32 signals at δ 1.80, 1.82, 1.825, 1.87, 1.90, 1.92, 1.97, 2.14, 2.15, 2.17, 2.20, 2.26, 2.32, 2.34, 2.49, 2.52 (16 Me out of maximum 20), 3.29, 3.53 (MeO), 6.58, 6.62, 6.65, 6.72, 6.74, 6.81, 6.93 (7 ArH out of maximum 10). Anal. Calcd for $C_{32}H_{38}O_3$: C, 81.66; H, 8.14. Found: C, 81.74; H, 8.40%.

3d: λ_{max}(hexane): 213 nm (log ϵ 4.60), 240.5 (4.32), 280 (4.18). ^{1}H NMR ($CDCl_3$) shows two diastereomers in a 2.3 ratio, and 24 signals. δ: 1.80, 1.815, 1.82, 1.84, 1.87, 1.90, 1.93, 1.95, 2.15, 2.20, 2.245, 2.25, 2.31, 2.32, 2.45, 2.46 (Me), 3.56, 3.73 (MeO), 6.57, 6.615, 6.62, 6.76, 6.81, 6.90 (ArH). Anal. Calcd for $C_{32}H_{38}O_3$: C, 81.66; H, 8.14. Found: C, 81.61; H, 8.36%.

JO9910435

(10) Okamoto, Y.; Kaida, Y.; Hayashida, H.; Hatada, K. *Chem. Lett.* **1990**, 909.

(11) Fritsch, R.; Hartmann, E.; Andert, D.; Mannschreck, A. *Chem. Ber.* **1992**, *125*, 849.